Holistic Design of a 2-Bladed Spar-Buoy Floating Offshore Wind Turbine

Holistic Design of a 2-Bladed Spar-Buoy Floating Offshore Wind Turbine

A Croce[1], **M Galliani**[1]

[1]Department of Aerospace Science and Technology, Politecnico di Milano, Milan, Italy

E-mail: alessandro.croce@polimi.it

Abstract. Floating offshore wind turbines require integrated design strategies due to the strong coupling between rotor aerodynamics, control, structural response, and the floating support system under combined environmental loading. This work extends a multidisciplinary wind turbine design framework originally developed for land-based applications to offshore concepts by explicitly including a spar-type floating platform, catenary mooring lines, and anchors within a nested, multi-level optimization workflow. The methodology is demonstrated on a 10 MW two-bladed spar-based concept by redesigning a three-bladed land-based concept. For the two-bladed configuration, the blade constraint is reformulated as a tip–tower clearance requirement to account for platform motions and teeter rotation. Results show that aerodynamic co-design induces coupled rotor–spar modifications, reducing the spar draft and mass. While spar geometry is only slightly modified during final sizing, mooring sizing is significantly affected once ultimate loads from dynamic simulations are enforced.

1. Introduction

The design of floating offshore wind turbines (FOWTs) presents significant challenges due to the complex environmental conditions in which they operate, including wind, waves, and currents. An integrated design approach aims to align the rotor, tower, and floating substructure with these external factors, seeking the optimal configuration to minimize the Levelized Cost of Energy (LCoE).

In recent years, the offshore wind industry has shifted from conventional design methods—where individual components were developed in isolation—towards an integrated design approach. This state-of-the-art methodology considers the turbine as a complete system, optimizing each component in relation to the others to maximize overall performance, reliability, and cost-efficiency ([1]).This integrated approach is crucial for ensuring the long-term viability of offshore wind farms, reducing operational and maintenance costs, and driving the industry towards large-scale deployment.

In the previous work ([2]), the authors presented a novel holistic design where a three-bladed rotor and the tower are designed together with a spar-type floater platform.

This approach, which considers from the very beginning of the design phase all the main components of the floating wind turbine, is here further developed and tested on a multi-megawatt upwind teeter-hinge two-bladed rotor.

2. Methodology

This work builds on a decade of advancements in multidisciplinary design technologies for land-based wind turbines (see [3], [4], and references therein). The holistic design framework utilizes nested optimization problems to integrate aerodynamic and structural design of both rotor and tower, with the main objective of minimizing the Levelized Cost of Energy.

In this study, the *classical* land-based wind turbine design approach has been extended to include offshore-specific components, namely the floating platform, the catenary mooring lines, and the anchors, within the overall design loop. To this end, the nested optimization problems shown in Figure 1 have been revisited to account for the strong coupling between the rotor and the floating substructure design.

To address different levels of design detail, wind turbine models of varying fidelity are used, ranging from reduced-order models for static aero-hydro-structural assessments to fully coupled aero-servo-hydro-elastic multibody models for time-domain load calculations.

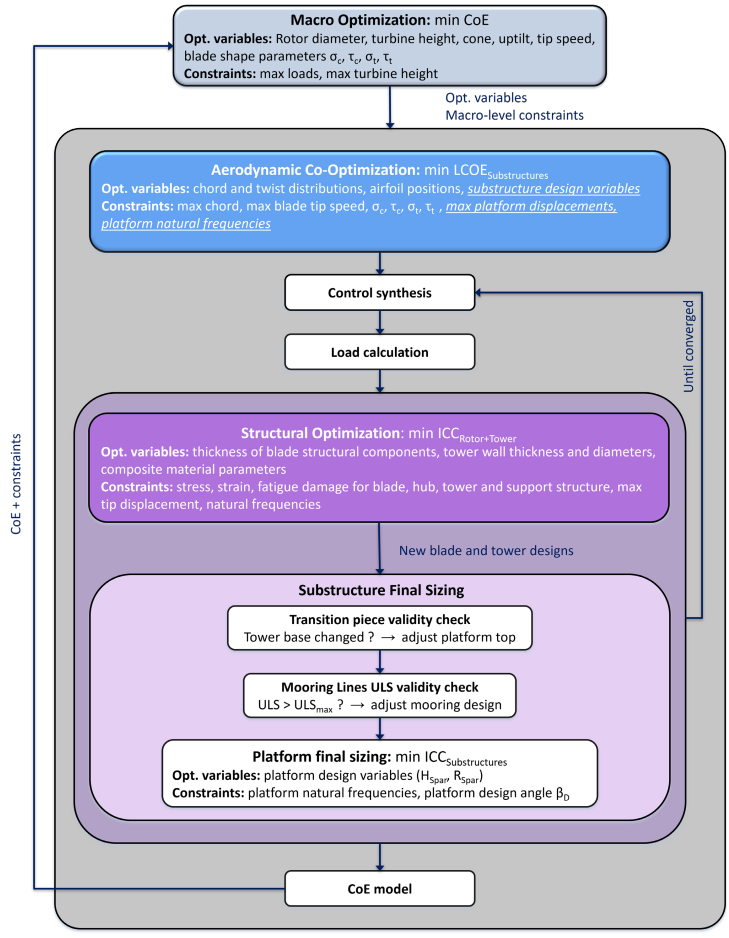

Figure 1. Cp-Max (Code for Performance Maximization) workflow scheme.
(σ_c – Rotor solidity; τ_c – Rotor tapering; σ_t – Thickness solid area; τ_t – Thickness weighted area [4]).

The workflow shown in Figure 1 includes the following main steps: i) an aerodynamic co-design phase, in which the rotor aerodynamic shape is optimized together with the floating support structure; ii) a model-based controller design and load assessment, based on certification-standard Design Load Cases; and iii) a structural sizing phase of the blade and tower components,

followed by an update of the floating support structure initially designed in the first design loop.

The simulations are performed using the aero-servo-hydro-elastic multibody solver *Cp-Lambda* (see, for details, [2] and [5] and references within).

2.1. Aerodynamic Co-Design

Typically, the land-based wind turbine design loop starts with a purely aerodynamic optimization ([3]). In this work, the presence of a floating platform makes it necessary to rethink this starting point. The rotor aerodynamic thrust has a strong impact on the floating platform design and vice versa (i.e., a significant platform pitch angle affects the aerodynamic performance). For this reason, the first optimization loop has been reformulated as a co-design phase, in which both the external shape of the rotor and that of the spar are treated as design variables. Consequently, the merit function has been updated from the original Annual Energy Production (AEP) to a simplified cost of energy ($LCoE_{\text{substructure}}$), which accounts for the substructure costs, while the internal blade geometry and the tower are kept fixed at this stage. However, the rotor blades and the tower have their own flexibility, which, in the initial loop, is that of the baseline designs. In so doing, the calculation of the aerodynamic coefficients takes into account the deformation of both these subsystems.

Accordingly, the design variables now include not only the parameters describing the blade chord and twist distributions, but also those characterizing the floating subsystem, collected here in the following parameter vector

$$\mathbf{p}_{\text{sub}} = [\mathrm{H}_{\text{Spar}},\ \mathrm{R}_{\text{Spar}},\ \mathrm{d}_{\text{Mooring}},\ \mathrm{r}_{\text{Mooring}},\ \mathrm{s}_{\text{Mooring}},\ \mathrm{z}_{\text{Fairlead}}], \tag{1}$$

where the components represent, respectively, the platform draft and radius, the equivalent diameter of the mooring lines, the mooring layout radius, the (non-dimensional) portion of the mooring line resting on the seabed, and the fairlead attachment height.

2.2. Control Synthesis and Load Calculation

Once the aerodynamic blade geometry and the floating platform have been optimized in the previous loop, a full aero-servo-hydro-elastic model of the floating wind turbine is set up, and Design Load Cases (DLCs) are simulated in accordance with the IEC Standards ([6]).

In this study, a relatively short list of DLCs has been selected based on the authors' experience in blade design, primarily to limit the computational cost within the scope of this work. These DLCs are representative of the relevant ultimate and fatigue design loads and are reported in Table 1, together with the corresponding safety factors and associated wind and wave conditions. These simulations include normal operating conditions under turbulent wind (DLCs 1.1, 1.2, 1.3, and 1.6), with wind speeds ranging from cut-in ($V_{in} = 3m/s$) to cut-out ($V_{out} = 25m/s$), as well as an extreme parked condition (DLC 6.1) at the reference wind speed ($V_{ref} = 50m/s$), which also accounts for wind–wave misalignment.

A model-based pitch–torque control law is automatically updated as part of the design process, as described, for instance, in [7].

Operative Condition	DLC	Wind Type	Wind Speed	Wave Type	Yaw Mis.	Wave Mis.	Safety Factor
Power Production	1.1	NTM	$V_{in} : V_{out}$	NSS	-	-	1.35
Power Production	1.2	NTM	$V_{in} : V_{out}$	NSS	-	-	1.00
Power Production	1.3	ETM	$V_{in} : V_{out}$	NSS	-	-	1.35
Power Production	1.6	NTM	$V_{in} : V_{out}$	SSS	-	-	1.35
Parked	6.1	EWM	V_{ref}	ESS	-8°/0°/+8°	-30°/0°/+30°	1.35

Table 1. List of selected Design Load Cases (DLCs) from the International Standards [6] (NSS - Normal Sea State; SSS - Severe Sea State; ESS - Extreme Sea State; NTM - Normal Turbulence Model; ETM - Extreme Turbulence Model; EWM - Extreme Wind speed Model).

2.3. Structural Design

In this final module, the blade internal geometry and the tower are first sized based on the load analysis performed in the previous step. The merit function of this loop mainly consists of the blade and tower Initial Capital Cost ($ICC_{\text{rotor+tower}}$), while the external blade geometry and the spar are kept fixed as computed in Section 2.1.

Accordingly, the design variables include the parameters describing the thickness distributions of the blade internal sub-components (shell, spar caps, shear webs, and reinforcements), as well as the tower diameter and thickness, as described in [4].

2.4. Substructure Final Sizing

This module has been developed specifically for offshore applications and is intended to adjust, rather than size, the floating system. During the final structural optimization phase, the floating substructures are resized in response to system mass adjustments while meeting Ultimate Limit State (ULS) constraints. Specifically, the transition piece connecting the tower to the spar is first adjusted to account for the optimized external diameter and thickness at the tower base. Subsequently, the mooring line diameter is adjusted based on the most restrictive constraint arising from the ultimate load analysis. Finally, a simplified optimization problem is solved to adjust the spar draft and radius, with the objective of re-establishing the buoyancy equilibrium of the overall system following the mass variations of the rotor, tower, and mooring lines.

3. Two-bladed blade to tower constraints

In the case of a two-bladed rotor configuration, the adoption of a teeter hinge became necessary. This design choice requires a reconsideration of the conventional blade tip deflection constraint, which in most glass-fiber-reinforced polymer (GFRP) blades primarily dictates the spar cap sizing ([7]) to ensure adequate structural stiffness. Under floating support conditions and a teeter rotor, however, the constraint is more appropriately expressed as the minimum allowable clearance between the blade and the tower, thereby accounting for the substantial tower displacements induced by, potentially large, platform motions and the teeter rotation.

For this reason, the classical blade deflection constraint ([4]) has been reformulated for the present two-bladed floating application. As in the previous approach ([7]), the clearance constraint is considered satisfied when negative values are obtained and is computed as:

$$C_{\text{tip}} = \frac{MinClearAllowed - Tip2Tower}{MinClearAllowed},$$

where the minimum allowed clearance ($MinClearAllowed$) is computed for each operating condition by its specific displacement safety factor (i.e. 70% for spinning load cases and 95% in

parked conditions). The minimum clearance ($Tip2Tower$), defined as the smallest distance between the blade tip and the tower reference point, is evaluated from the dynamic time histories for all blades over the entire simulation time.

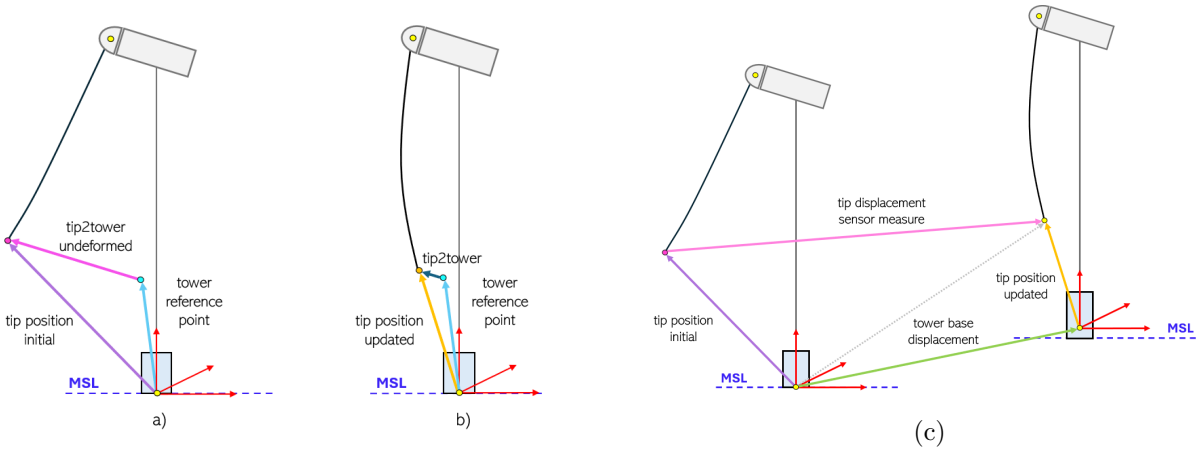

Figure 2. Visualization of the C_{tip} computation (left) and of the tower base displacement correction (right).

Specifically, it is determined through a vector operation that involves three variables, one of which is the relative position of the blade tip ($TipDisplacementSensorMeasure$), measured by a sensor in the tower inertial frame with respect to the blade tip initial configuration.

In the context of floating offshore wind turbines, as the platform moves in surge, sway, and heave directions, this relative measurement must be corrected for these additional motions to obtain the correct updated position of the blade tip ($TipPositionUpdated$). The vector procedure is illustrated in Figure 2c, where the updated tip position is identified and subsequently used in the clearance calculation, as shown in Figure 2b. The C_{tip} constraint is then evaluated for each Design Load Case (DLC), and the operating condition exhibiting the least compliant clearance constraint is identified. The corresponding information, including platform base motions, is then stored and used in the iterative blade sizing process in the *Structural Optimization* loop (Figure 1). From this point onward, the procedure follows the previous implementation up to the start of the blade structural sizing, where the associated clearance evaluation process was reformulated in the inertial reference frame and adapted for floating applications. The procedure begins by reconstructing the blade tip updated position ($TipPositionUpdated$) corresponding to the previously identified critical condition through a sequential superimposition of effects, as illustrated in Figure 3, which are applied to the blade tip initial position ($TipPositionInitial$) in the following order: blade deflection, teeter, roll, pitch, and yaw rotations.

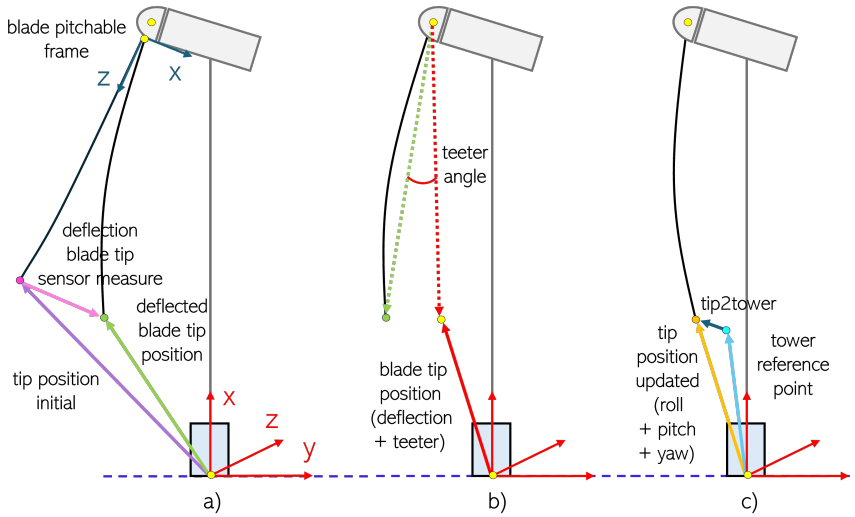

Figure 3. Superimposition of effects sequence.

During the iterative process, the corresponding C_{tip} constraint is then evaluated using the computed clearance ($Tip2Tower$) together with the previously stored minimum admissible clearance ($MinClearAllowed$). If not compliant, to satisfy the tip–tower clearance requirement, the blade deflection is adjusted by modifying the blade internal structure.

This implementation does not account for the flexibility of the tower top, which can reasonably be assumed to vibrate, thereby contributing to the blade tip movement, but the procedure as it is now is considered acceptable nonetheless.

4. Results and Discussion

To demonstrate this multi-disciplinary and multi-nested design methodology, a classic 10-MW turbine on a spar platform has been re-designed with a two-bladed teeter-hinged rotor.

4.1. Baseline

The optimization loops adopted in this work are all gradient-based and require initial guesses from which to start the iterations. This choice, while potentially limiting the exploration of globally optimal solutions—possibly including designs that are difficult to realize—allows, on the other hand, the description of complex geometries (such as the chord distribution) using a limited number of degrees of freedom and enables, for instance in an industrial context, the use of previous design solutions as starting points.

In this work, the baseline wind turbine considered is based on a 10 MW three-bladed rotor originally designed for land-based applications [3] with an adapted tower (i.e., a tower structure adjusted for this offshore case). Moreover, a conservative spar platform was preliminarily designed starting from literature data by applying the procedure described herein outside an optimization framework. The rotor characteristics are reported in Table 2, together with the six design variables used to parametrize the floating system. Figure 4b shows the mesh and geometry of the 120 m spar draft used for the baseline.

For the two-bladed configuration, a teeter hinge was introduced in the wind turbine model. Its operating range, together with the associated restraint torque, was defined based on the work presented in [5]. In the same study, to compensate for the negative impact on power extraction and aerodynamic performance resulting from the removal of one blade, the two-bladed rotor solidity was increased by 16% by modifying the chord distribution of the three-bladed baseline as shown in Figure 4a.

Variable	Value
Rated electrical power	10 MW
Wind class	IEC 1A
Rotor diameter	178.3 m
Rotor cone angle	6.5°
Nacelle uptilt angle	7.0°
Rotor overhang	7.07 m
Prebend	5.94 m
Hub height	119 m
Tower height	115.63 m
H_{spar}	120 m
R_{spar}	9 m
$d_{mooring}$	0.177 m
$r_{mooring}$	855.2 m
$s_{mooring}$	0.177
$z_{fairlead}$	-77.2 m

Table 2. Main *Baseline* data.

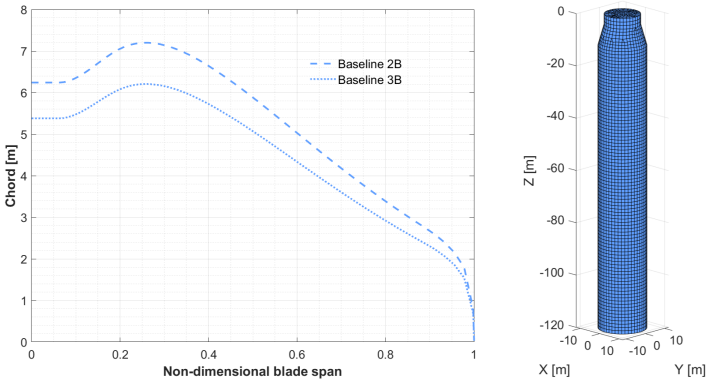

(a) *Baseline* chord distributions **(b)** Spar mesh

Figure 4. *Baseline* blade and spar visualization.

4.2. Aero Co-Design

Starting from the previously defined baseline, several analyses were carried out for two- and three-bladed rotors by modifying the rotational speed limit and other design parameters. In the following, the case of a two-bladed rotor with no constraint on the rotational speed is reported, i.e. without any limitation on the blade tip speed and, consequently, on noise emissions. Further analysis and comparisons with a three-bladed rotor are out of the scope of this work and will be presented in future papers.

All optimizations were performed using the MATLAB gradient-based optimizer `fmincon` with the `active-set` algorithm, which iteratively identifies the active constraints and searches for a local minimum of the constrained nonlinear multivariable objective function. To facilitate the optimization and ensure a smooth iterative procedure, a pre-optimization check is carried out to verify that the initial design (i.e., the baseline) satisfies all constraints. If necessary, a feasible initial point is obtained by solving the same optimization problem with a zero-cost objective function. This procedure is applied at the beginning of both the aero co-design and the structural optimization phases. In this procedure, all gradients are computed numerically.

The initial focus of the multi-level formulation is the *Aero Co-Design* of the blade external geometry together with the floating substructure. Regarding the aerodynamic rotor design variables, during this phase the chord and twist distributions are optimized, with control points set at $\eta_c = [0.2, 0.4, 0.6, 0.8, 0.9]$ and $\eta_t = [0, 0.1, 0.2, 0.4, 0.6, 0.8, 1]$ for chord and twist, respectively. At the same time, the vector of substructure design parameters is defined by the six unknowns described in Eq. 1.

The optimization of the blade thickness distribution is also possible; however, for these initial tests, this design variable was kept fixed in order to limit the computational demand. As a result, the airfoils are maintained at fixed spanwise positions along the blade.

The aerodynamic co-design results reveal substantial design modifications, particularly in the rotor aerodynamic shape and, concurrently, in the spar geometry. Figure 5 shows the chord and twist distributions obtained from this optimization loop: the rotor solidity is slightly reduced, leading to a decrease in aerodynamic performance (and cost, as shown in Table 3); however, at the same time, the spar draft is reduced to approximately 100 m, as shown in Figure 6b and in Table 4. This outcome arises because the optimizer, whose objective is to minimize the substructure levelized cost of energy ($LCoE_{\text{substructure}}$), identifies the best compromise between the

Annual Energy Production of the rotor and the mass (i.e., cost) of the floating substructure. This trade-off can also be observed in Table 3, where $LCoE_{\text{substructure}}$ is reduced by approximately 13%, the AEP by about 0.3%, and the substructure costs ($C_{\text{substructure}}$) by 20.5%.

Moreover, Tables 3 and 4 show that the reduction in platform draft (H_{spar}) leads to a higher center-of-gravity location (Z_{CoG}), while the spar radius (R_{spar}) increases only slightly. Regarding the mooring system, both the chain diameter ($\text{d}_{\text{mooring}}$) and the mooring layout radius ($\text{r}_{\text{mooring}}$) decrease significantly, whereas the portion of the mooring line resting on the seabed ($\text{s}_{\text{mooring}}$) increases. Concurrently, the fairlead vertical position ($\text{z}_{\text{fairlead}}$) is shifted upward, mitigating the pitch overturning moment generated by the restoring forces of the mooring lines.
As the total mooring line length ($\text{l}_{\text{mooring}}$) is the sum of the suspended line length (not reported here), and the actual length of the portion resting on the seabed ($\text{r}_{\text{mooring}} \cdot \text{s}_{\text{mooring}}$), the observed changes in the design parameters indicate that, during this initial design phase, the optimizer tends to limit mooring line deployment, as illustrated in Figure 7 and reported in Table 4.

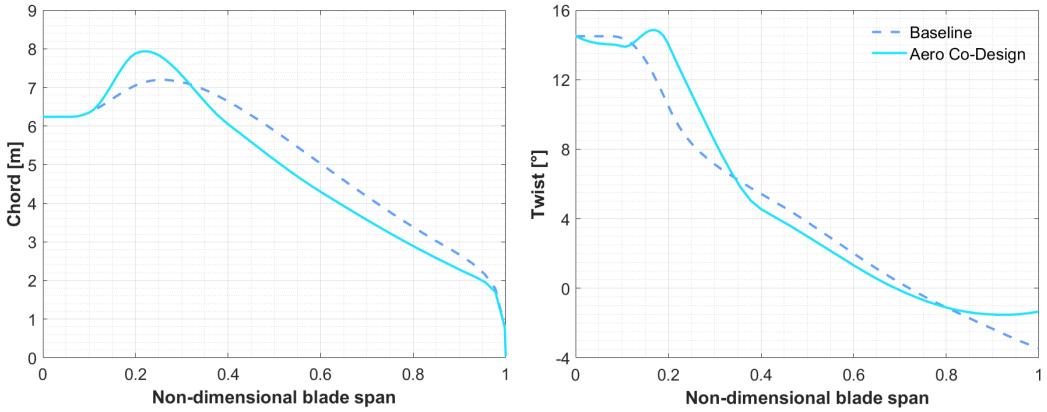

Figure 5. Chord and twist distributions from the *Aero Co-Design* compared to the *Baseline* ones.

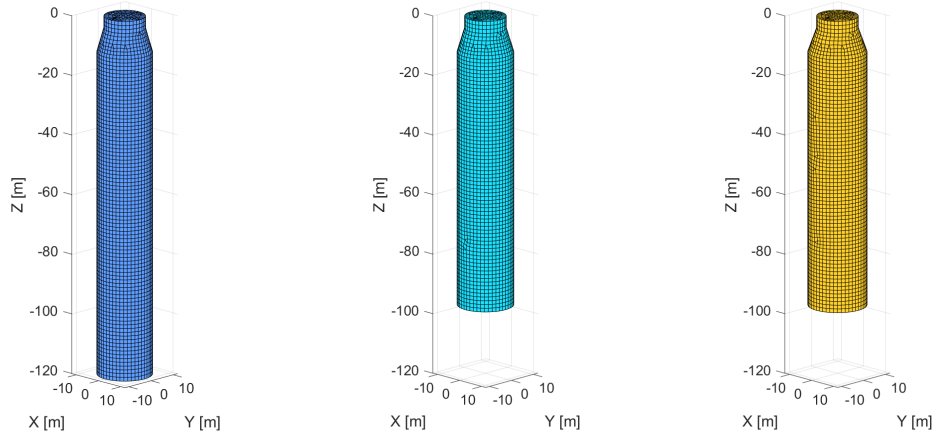

(a) *Baseline* (b) *Aero Co-Design* (c) *Final Design*

Figure 6. Spar geometry: visual comparison between the *Baseline*, the *Aero Co-Design* and the *Final Design* optimization loop.

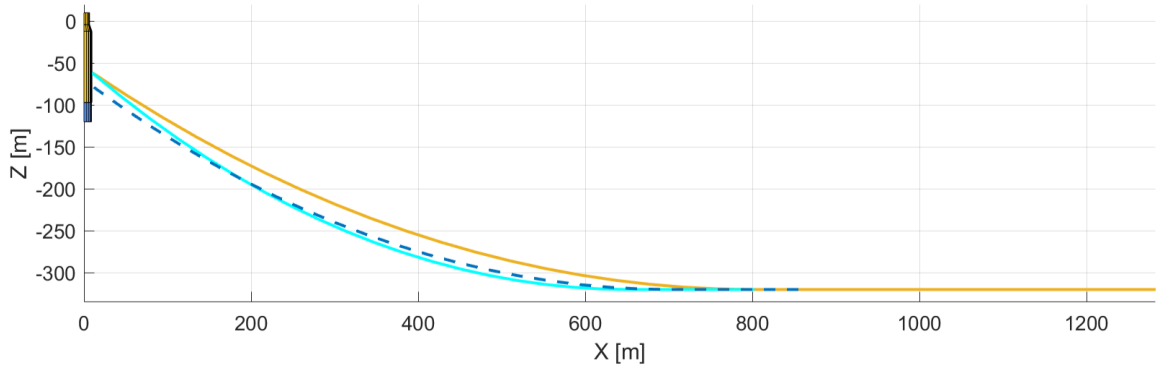

Figure 7. Mooring line geometry: visual comparison between the *Baseline* (dotted blue line), the *Aero Co-Design* (solid light-blue) and the *Final Design* (dashed yellow) optimization loops.

Another important design parameter is the *platform pitch design angle* β_D, defined as a function of the resultant moment acting on the platform and the total system pitch stiffness. Hence, β_D represents a trade-off between the required floating pitch stiffness—and thus substructure material consumption—and aerodynamic performance. In other words, it can be interpreted as the maximum rotor tilt angle that the system can accommodate before excessively compromising power output. For this reason, the aerodynamic co-design optimization inherently leads to an optimal platform pitch design angle, which is then used as a reference condition for the subsequent structural evaluation. The (sub-optimal) baseline model exhibits a design pitch angle of $\beta_D = 4°$, whereas the final value obtained from the aerodynamic co-design is $\beta_D = 6.7°$.

	$LCoE_{substructure}$	AEP_{stat}	C_{blade}	C_{tower}	$C_{substructure}$	β_D	z_{CoG}	z_{CoB}
	[€/MWh]	[GWh]	[k€]	[M€]	[M€]	[°]	[m]	[m]
Baseline	65.65	45.41	233.89	4.936	29.81	4.00	-95.0	-61.7
Aero Co-Design	52.50	45.12	230.09	4.936	23.69	6.70	-76.7	-50.22
Final Design	–	44.31	262.71	4.936	26.55	6.74	-77.1	-50.45

Table 3. Comparison of selected rotor, tower and floating support system costs and design parameters.

	H_{spar}	R_{spar}	$d_{mooring}$	$r_{mooring}$	$s_{mooring}$	$z_{fairlead}$	$l_{mooring}$
	[m]	[m]	[m]	[m]	[–]	[m]	[m]
Baseline	120.0	9.00	0.177	855.20	0.177	-77.20	899.4
Aero Co-Design	96.8	9.17	0.129	802.34	0.186	-61.50	857.4
Final Design	96.9	9.58	0.141	1282.5	0.374	-61.50	1326.1

Table 4. Comparison of the floating support system design parameters and total mooring line length.

4.3. Structural Design

Following the aerodynamic co-design, a pitch–torque control law is synthesized and dynamic simulations are performed in accordance with the International Standards, as described, for example, in [7] and showed in Figure 1. The ultimate and fatigue loads arising from these dynamic simulations, together with the wind turbine frequencies and blade to tower clearance (as described in the previous Section 3) concur to compute the structural design constraints (see, for instance, [7]) used in the *Structural Design* phase.

The *Structural Design* loop keeps the aeroelastic loads frozen while minimizing its specific merit function which mainly consists of the blade and tower ICC and satisfying the design constraints. Once the optimization problem has converged, as shown in Figure 1, the aeroelastic loads—together with the control synthesis—are re-computed, and this structural optimization is restarted. This iterative process is concluded when the blade and tower masses reach convergence within a prescribed tolerance. For the specific problem considered here, convergence is typically achieved within two to four iterations.

Figure 8 shows, for instance, the final thickness distributions of the spar caps and external blade skin. As expected, the structural blade and tower masses increase in the *Structural Design* loop compared to both the Baseline and the *Aero Co-Design* cases.

For this specific study, the tower structure is not modified with respect to the baseline one and is therefore not presented. This behavior can be observed from the tower costs reported in Table 3. This is likely because the structural constraints are already satisfied at the initial iteration and because the tower mass (and associated cost) has a relatively small weight in the merit function compared to other cost components. The impact of the tower—particularly in terms of its natural frequencies—will be further investigated and presented in a future works.

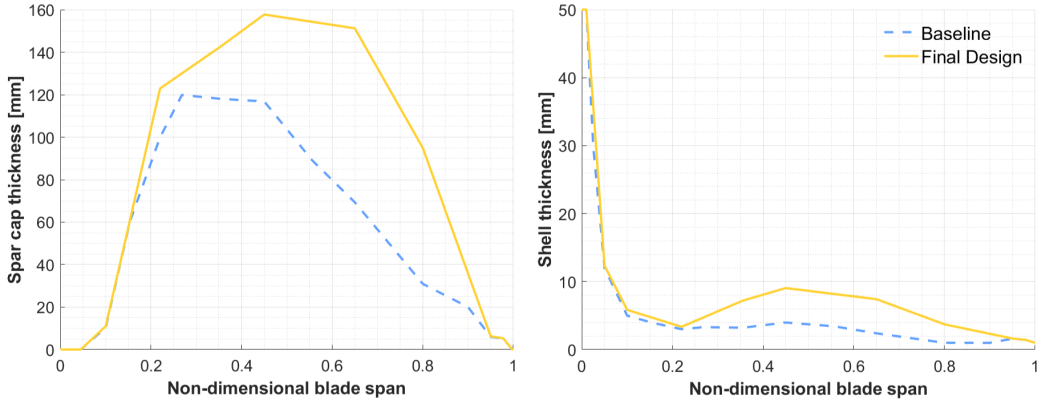

Figure 8. Blade structural element thicknesses distributions.

4.4. Final Sizing

At the end of the blade and tower design phase, the floating substructure is verified and, if necessary, automatically updated. Several design constraints (see [2]) are enforced at this stage, together with the floating pitch design angle β_D, which is constrained to remain equal to the previously obtained optimal value within a prescribed tolerance. As shown in Tables 3 and 4, as well as in the visual comparison of Figure 6, the spar geometry is only slightly modified, indicating that the strong coupling between the rotor aerodynamics and the spar geometry accounted for in the *Aero Co-Design* phase is able to capture most of the relevant effects.

The situation is different for the mooring system, mainly because the ultimate loads computed during the *Structural Design* loop are used to size these components, together with the anchors. Therefore, the total mooring line length of the *Final Design* increased significantly compared to the *Baseline* and *Aero Co-Design*, as shown in Figure 7 and Table 4. However, the smaller final mooring line diameter relative to the *Baseline Design* helps balance the mooring system costs. Overall, the results underline the importance of including verifications based on dynamic load calculations, which are deliberately not included in the initial co-design phase in order to limit the computational cost of the global optimization process, but are instead accounted for in the final sizing of the substructure. It is worth noting that the mooring system sizing is currently based on ultimate loads, while cumulative fatigue damage loads are monitored

but not yet included in the sizing process. Finally, the ballast mass is adjusted to restore the buoyancy equilibrium of the overall system.

5. Conclusions

This paper presents a novel approach for the integrated design of offshore wind turbines aimed at reducing the LCoE. The proposed methodology couples the aerodynamic and structural design of the rotor with the design of its support structure (floater, mooring lines, and anchors).

The 10 MW two-bladed teeter-hinge case demonstrates the relevance of formulation choices specific to floating applications: replacing the classical blade tip deflection constraint with a tip–tower clearance constraint enables consistent sizing in the presence of platform motions and teeter rotation. The aerodynamic co-design results in coupled rotor–spar modifications that reduce the spar draft to approximately 100 m and increase the platform pitch design angle from $\beta_D = 4°$ to $\beta_D = 6.7°$, reflecting a clear trade-off between floating-system stiffness/material demand and aerodynamic performance. In quantitative terms, the co-design phase achieves a reduction of about 13% in the simplified $LCoE_{\text{substructure}}$, with only a minor decrease in (static) AEP ($\sim 0.3\%$) and a substantial reduction in substructure costs ($\sim 20.5\%$). The final sizing stage confirms that spar geometry requires only limited adjustments, suggesting that the early rotor–spar coupling is largely captured by the co-design formulation. Conversely, mooring and anchoring components are more sensitive to dynamic verification, since ultimate loads from DLC simulations significantly affect their sizing; fatigue damage is currently monitored but not yet included as a sizing driver.

Future work will focus on (i) systematically quantifying the role of tower dynamics and frequency placement relative to blade-pass excitations—particularly relevant for two-bladed rotors—and (ii) extending mooring/anchor sizing to explicitly include fatigue-driven criteria within the holistic optimization process.

Acknowledgements

The authors would like to thank Kutay Yilmazlar, who developed much of the code that led to this work in his doctoral thesis.

References

[1] Patryniak K, Collu M and Coraddu A 2022 Multidisciplinary design analysis and optimisation frameworks for floating offshore wind turbines: State of the art *Ocean Engineering* **251** 111002

[2] Croce A and Yilmazlar K 2025 Integrated aero-hydro-structural design of a 10-mw spar-type floating wind turbine *Wind Energy Science - to be submitted*

[3] Croce A, Cacciola S and Sartori L 2022 Evaluation of the impact of active wake control techniques on ultimate loads for a 10mw wind turbine *Wind Energy Science* **7** 1–17

[4] Sartori L, Bellini F, Croce A and Bottasso C 2018 Preliminary design and optimization of a 20mw reference wind turbine *Journal of Physics: Conference Series* **1037**

[5] Civati M, Sartori L and Croce A 2018 Design of a two-bladed 10 mw rotor with teetering hub *Journal of Physics: Conference Series* **1037** 042007

[6] IEC 2019 Wind energy generation systems - part 3-2: Design requirements for floating offshore wind turbines *Technical Specification (TS)* **IEC TS 61400-3-2:2019**

[7] Croce A, Sartori L, Lunghini M, Bortolotti P and Bottasso C 2016 Lightweight rotor design by optimal spar cap offset *Journal of Physcs: Conference Series* **753**